Targeted repression of essential genes to arrest growth and increase carbon partitioning and biofuel titers in cyanobacteria

Kiyan Shabestary, Josefine Anfelt, Emil Ljungqvist, Michael Jahn, Lun Yao and Elton P. Hudson*

KTH—Royal Institute of Technology.
School of Engineering Sciences in Chemistry, Biotechnology, and Health,
Science for Life Laboratory,
Stockholm SE-171 21 Sweden.

*Correspondence to paul.hudson@biotech.kth.se

kiyan@kth.se
janfelt@kth.se
emilel2@kth.se
michael.jahn@scilifelab.se
lunyao@kth.se
paul.hudson@biotech.kth.se

Graphical abstract

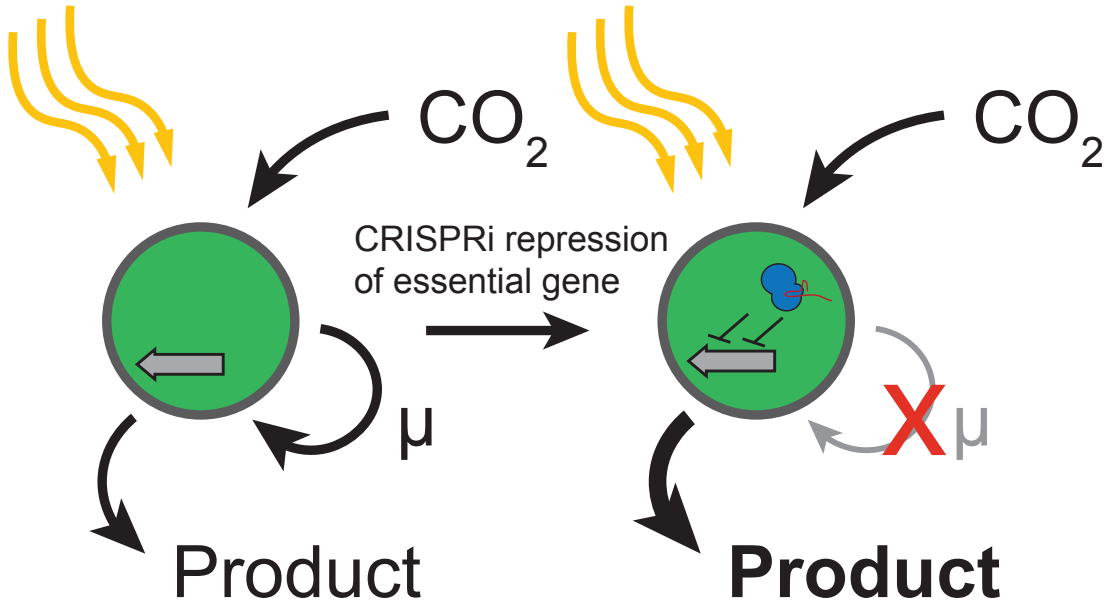

Abstract

Photoautotrophic production of fuels and chemicals by cyanobacteria typically gives lower volumetric productivities and titers than heterotrophic production. Cyanobacteria cultures become light limited above an optimal cell density, so that this substrate is not supplied to all cells sufficiently. Here, we investigate genetic strategies for a two-phase cultivation, where biofuel-producing *Synechocystis* cultures are limited to an optimal cell density through inducible CRISPR interference (CRISPRi) repression of cell growth. Fixed CO_2 is diverted to ethanol or n-butanol. Among the most successful strategies was partial repression of citrate synthase *gltA.* Strong repression (>90%) of *gltA* at low culture densities increased carbon partitioning to n-butanol 5-fold relative to a non-repression strain, but sacrificed volumetric productivity due to severe growth restriction. CO_2 fixation continued for at least 3 days after growth was arrested. By targeting sgRNAs to different regions of the *gltA* gene, we could modulate GltA expression and carbon partitioning between growth and product to increase both specific and volumetric productivity. These

growth arrest strategies can be useful for improving performance of other photoautotrophic processes.

Keywords: Dynamic metabolic engineering, Cyanobacteria, Growth-arrest, Light availability, CRISPRi

The tradeoff between growth and specific productivity must be tightly regulated when producing compounds in microbial cell factories. If carbon partitioning towards product is too high, cellular density accumulates slowly, resulting in low volumetric productivity. Conversely, low specific productivities result in low yields since substrate is mainly converted to biomass. The ideal bioprocess would be divided into two parts: rapid biomass accumulation to an optimal cell density, and then rapid product synthesis with minimum or no biomass formation. In dynamic metabolic engineering, carbon flux to growth and production are altered during the bioprocess.[1,2] Flux alterations can be achieved by partially or completely repressing enzyme levels essential for biomass formation,[3] involved in glycolysis,[4–6] fatty acid synthesis (OPX Biotechnologies, US Patent application, US2010/8883464), terpenoid synthesis,[7] nucleobase synthesis or cell division.[8] The signal for switching between growth and production can be externally added, but is ideally generated *in situ*. Photoautotrophic production processes in particular would benefit from biomass repression since light shading at high cell densities can reduce specific and total productivities.[9,10]

The CRISPR-interference (CRISPRi) system has been recently ported to cyanobacteria, where it has been used to repress genes upon induction with external effector molecules.[11–14] CRISPRi could thus be a useful tool for an eventual two-phase cyanobacteria process. Here, we evaluate the effectiveness of CRISPRi to arrest cell growth and divert fixed CO_2 to biofuel in *Synechocystis* PCC6803 strains engineered to produce n-butanol and ethanol (Fig. 1). The ethanol production cassette contained a copy of the native *Synechocystis* alcohol dehydrogenase

(*slr1192*) and a pyruvate decarboxylase (*pdc*) from *Zymomonas mobilis* (Table 1). The n-butanol cassette contained a heterologous phosphoketolase (Xfpk) to increase acetyl-CoA pools[15] and a heterologous acetoacetyl-CoA synthase (NphT7) to impart thermodynamic driving to synthesize acetoacetyl-CoA from malonyl-CoA.[16] In an ethanol-producing strain (KS33, Table S1), we repressed *odhB*, an essential subunit of pyruvate dehydrogenase complex (PDH) to create KS92. PDH catalyzes the decarboxylation of pyruvate and formation of acetyl-CoA. The condition-dependent expression of *odhB* has been reported previously as a growth-control strategy for cyanobacteria (Joule Unlimited, US Patent application, US2012/0164705). In a butanol-producing strain (KS70, Table S1), we targeted citrate synthase (*gltA*) to create KS96. GltA consumes acetyl-CoA in the first step of the TCA cycle, an important route for α-ketoglutarate derived amino acids and other biomass precursors. Modulation of *gltA* expression through heterologous promoters, RBS libraries, or a protein degradation tag has been recently demonstrated to increase acetyl-CoA pools and biofuel production in *E. coli.*[5,17] In addition to these specific pathways, we tested repression of essential enzymes in nucleobase synthesis[8] (*pyrF,* KS93 and KS162) and nitrate uptake[18] (*nrtA,* KS94) as general growth-arrest strategies. All repression targets except *odhB* were confirmed as essential for growth using flux balance analysis (FBA) on a genome-scale model.[19] *In silico*, the native Xfpk reactions could bypass the PDH (*odhB*) knockout. *In vivo,* Xfpk could not rescue the growth-defect phenotype of *odhB* repression (Fig. 2A), indicating a low enzyme capacity. For each target, sgRNAs and dCas9 were under the tightly repressed, anhydrotetracycline (aTc) inducible promoter PL_{22}.[20]

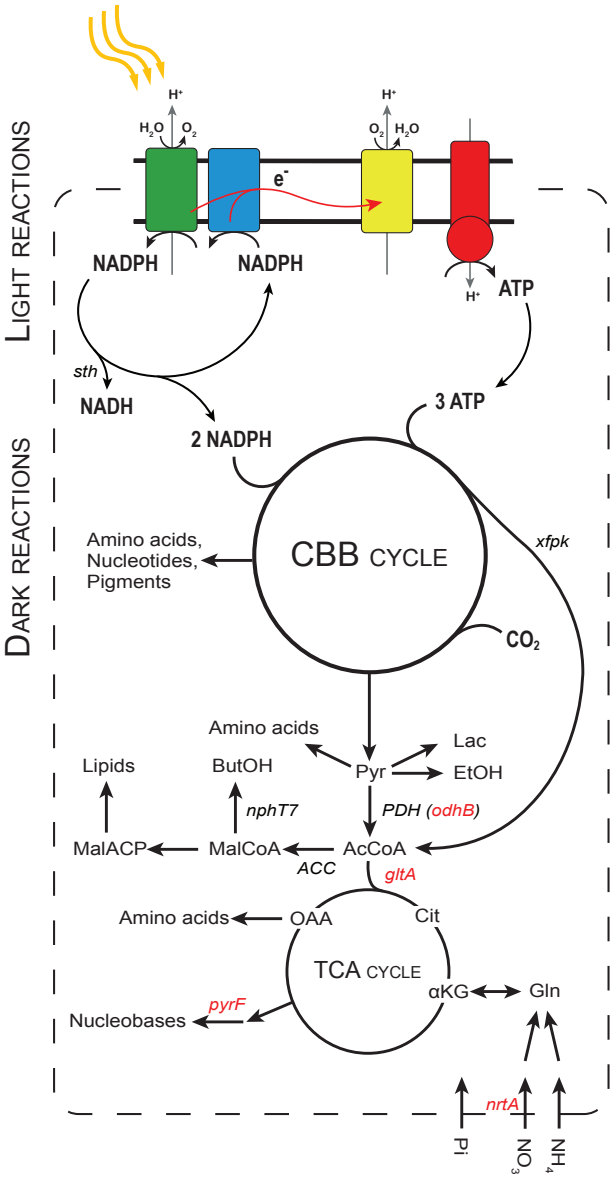

Figure 1. Simplified metabolic map of *Synechocystis* showing routes to butanol and ethanol production. Genes targeted for repression using CRISPRi in this study are indicated in red.

In first trials, CRISPRi-mediated knockdown was induced at low culture density (OD_{730} 0.1) and cultures monitored over 5 days (Fig. 2A,B). Repression of transcription of each gene was confirmed using RT-qPCR and was greater than 50% relative to non-induced cultures (Fig. S1). Repression of *gltA* (>90% repressed),

odhB (>50% repressed), and *pyrF* (>60% repressed) arrested cell growth (Fig. 2A,B). We also measured ethanol and butanol titers and calculated carbon partitioning for the growth repression strains. In all cases, product titers and specific productivities were lower when CRISPRi arrested growth due to a low cell density and cessation of CO_2 uptake and possible photoinhibition (Fig. 2C,D and Fig. S2). However, carbon partitioning to biofuel was higher when growth was arrested in KS92 (*odhB*) and KS96 (*gltA*), though error bars were large due to variability in the growth arrest (Fig. 2E,F). KS92 (*odhB*) and KS96 (*gltA*) had 2-fold and 5-fold higher carbon partitioning to ethanol and butanol, respectively, when growth was arrested. The strong effect from these targets is likely due to pyruvate and acetyl-CoA precursor build-up, in addition to repression of biomass formation. In KS93 and KS162 (*pyrF*), carbon partitioning was only mildly affected, likely because this repression target is not a metabolic branch point (Fig. 2E,F). The *nrtA* repression strain KS94 also had a significant increase in carbon partitioning to butanol (Fig. S3). However, a chlorosis (bleached) phenotype was observed due to the onset of internal nitrogen limitation, which rapidly stopped CO_2 uptake. Due to the 5-fold increase in carbon partitioning to butanol in KS96, we sought to optimize the timing and strength of *gltA* repression.

122 **Table 1.** Strains used in this study.

Strain	Pathway cassette	dCas9 cassette	sgRNA cassette
KS92	ΔslrO168::Ptrc adhA pdc KmR	ΔpsbA1::PL22 dCas9 SpR	Δslr2030-2031::PL22_sgRNA-odhB_184 odhB_318 CmR
KS93	ΔslrO168::Ptrc adhA pdc KmR	ΔpsbA1::PL22 dCas9 SpR	Δslr2030-2031::PL22_sgRNA-pyrF_12 pyrF_215 CmR
KS94	ΔslrO168::Ptrc pduP phaJ Ptrc ter phaB KmR, ΔphaA::Psca6-2 nphT7 xfpk GmR	ΔpsbA1::PL22 dCas9 SpR	Δslr2030-2031::PL22 sgRNA-nrtA_14 phaEC_95 CmR
KS96	ΔslrO168::Ptrc pduP phaJ Ptrc ter phaB KmR, ΔphaA::Psca6-2 nphT7 xfpk GmR	ΔpsbA1::PL22 dCas9 SpR	Δslr2030-2031::PL22 sgRNA-gltA_42 gltA_164 CmR
KS162	ΔslrO168::Ptrc pduP phaJ Ptrc ter phaB KmR, ΔphaA::Psca6-2 nphT7 xfpk GmR	ΔpsbA1::PL22 dCas9 SpR	Δslr2030-2031::PL22_sgRNA-pyrF_12 pyrF_215 CmR
KS87	ΔslrO168::Ptrc pduP phaJ Ptrc ter phaB KmR, ΔphaA::Psca6-2 nphT7 xfpk sth GmR	ΔpsbA1::PL31 dCas9 SpR	Δslr2030-2031::PL22 sgRNA-phaE_20 ackA_95 ndhD1_134 ndhD2_39 CmR
KS142	ΔslrO168::Ptrc pduP phaJ Ptrc ter phaB KmR, ΔphaA::Psca6-2 nphT7 xfpk sth GmR	ΔpsbA1::PL31 dCas9 SpR	Δslr2030-2031::PL22 sgRNA-gltA_463 ackA_21 phaEC_95 ndhD1_134 ndhD2_39 CmR
KS143	ΔslrO168::Ptrc pduP phaJ Ptrc ter phaB KmR, ΔphaA::Psca6-2 nphT7 xfpk sth GmR	ΔpsbA1::PL31 dCas9 SpR	Δslr2030-2031::PL22 sgRNA-gltA_762 ackA_21 phaEC_95 ndhD1_134 ndhD2_39 CmR

123

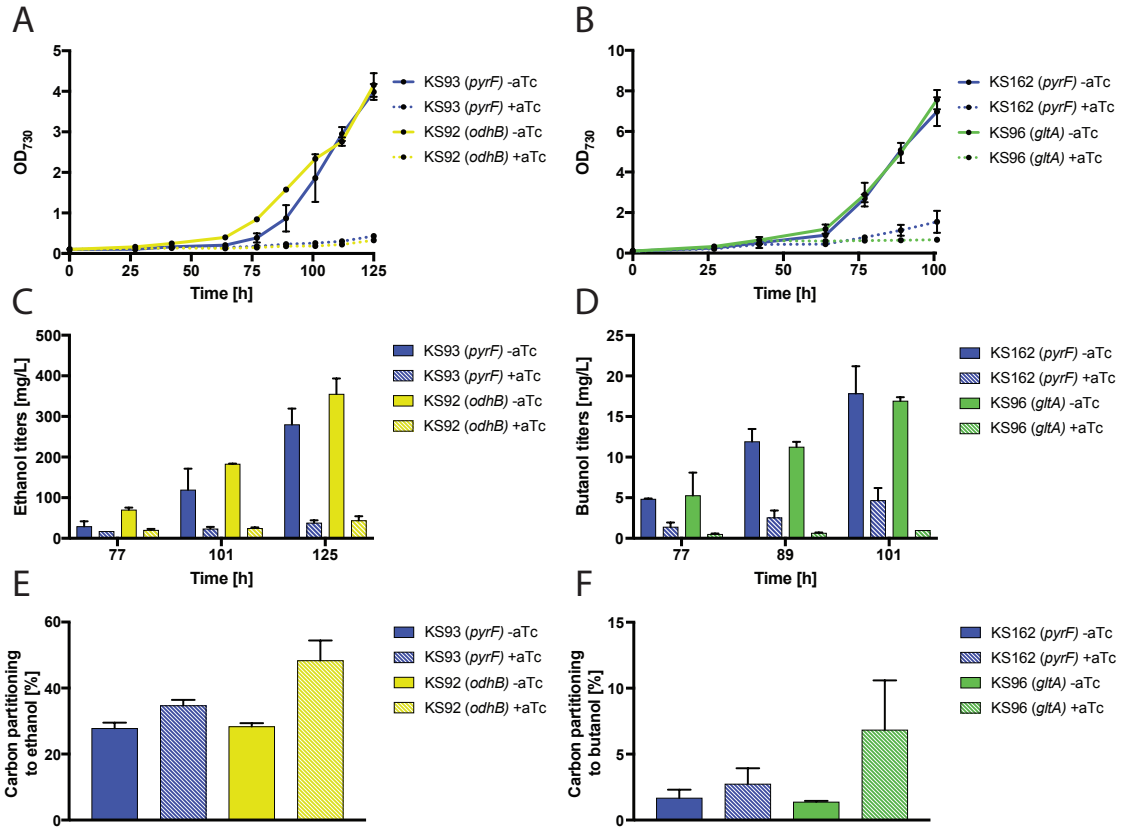

Figure 2. Effect of CRISPRi-mediated gene repression on *Synechocystis* growth, titer and carbon partitioning to biofuel. (A,B) Growth curves, (C,D) biofuel titers, and (E,F) average carbon partitioning to ethanol and butanol. Cultures were started in flasks at OD_{730} 0.1 with or without aTc, which induced CRISPRi. Butanol production was induced with IPTG at OD_{730} 0.4. Ethanol production was constitutive. Cultivations were performed in duplicate. Light intensity was 100 μE. Carbon partitioning to product was calculated as the flux going to product over the flux going to biomass and product in C-mol/gDCW/h (Supplementary Note).

We first aimed to increase volumetric butanol titers from KS96 by inducing *gltA* repression at higher cell densities. We tested induction at OD_{730} 0.1 (12 h after culture inoculation) and at OD_{730} 0.4 (18 h after). Induction at OD_{730} 0.1 prevented cells from reaching a high cell density (OD_{730} < 1.0) and butanol titers were lower than the non-induced culture (Fig. S4). Induction at OD_{730} 0.4 allowed cells to reach higher cell density (OD_{730} 4.0), and titers were 70% higher than the non-induced culture. Specific productivities also improved 2-fold (Fig. S4). These results show the importance of timing the growth arrest to achieve high specific and volumetric

productivity. In a recent study, the optimal cell density for photoautotrophic production was calculated to be 0.76 gDCW/L corresponding to approximately OD_{730} 2.0.[9,15] To stop growth at the optimal cell density, one must consider the delay between CRISPRi induction and effect, as GltA protein already present in the cell must be diluted or degraded. To reduce such a delay, a protease degradation sequence could be added to GltA.[21]

One complication with a growth-arrest production strategy is that substrate uptake may be linked to growth. Growth repression due to nutrient limitation or repression of biomass formation has been shown to reduce metabolic activity in heterotrophs, often in the form of reduced glucose uptake.[6,8,22] A recent study showed decreased photosynthetic activity and ethanol production by *Synechocystis* when growth stalled in stationary phase.[10] We measured CO_2 uptake in KS96 (*gltA*) grown in a batch photobioreactor with and without growth arrest (Fig. 3A,B).[23] At the early stages of cultivation (38 h), before the onset of light limitation, the induced KS96 (*gltA*) had a higher specific CO_2-uptake rate, perhaps indicative of a sink effect on CO_2 uptake as carbon is routed to butanol.[24] At 62 h (2.5 d) post-induction, cell growth was completely arrested, though CO_2 fixation continued for at least 2 more days. At 111 h (4.5 d) post-induction, the specific CO_2 uptake rate in the growth-arrested culture had dropped to 25% of its initial value. It was clear that butanol synthesis alone could not sustain high CO_2 uptake for an extended time once growth was arrested. It is possible that an accumulation of metabolic intermediates signals CO_2 uptake to cease, or at least some flux through GltA is required to repair damaged proteins so that the metabolic rate can be maintained. One hypothesis is

that the cell becomes over-reduced without biomass formation as a reductant sink. We measured NADPH at two time points during growth arrest and found that it was at least 2-fold higher than when cells were not growth arrested (Fig. 3C). The specific CO_2 uptake rate in the control culture also decreased with time, due to light shading at high cell densities. We note that the volumetric CO_2 uptake rates were lower in the growth-arrested culture due to a lower cell density (Fig. S5).

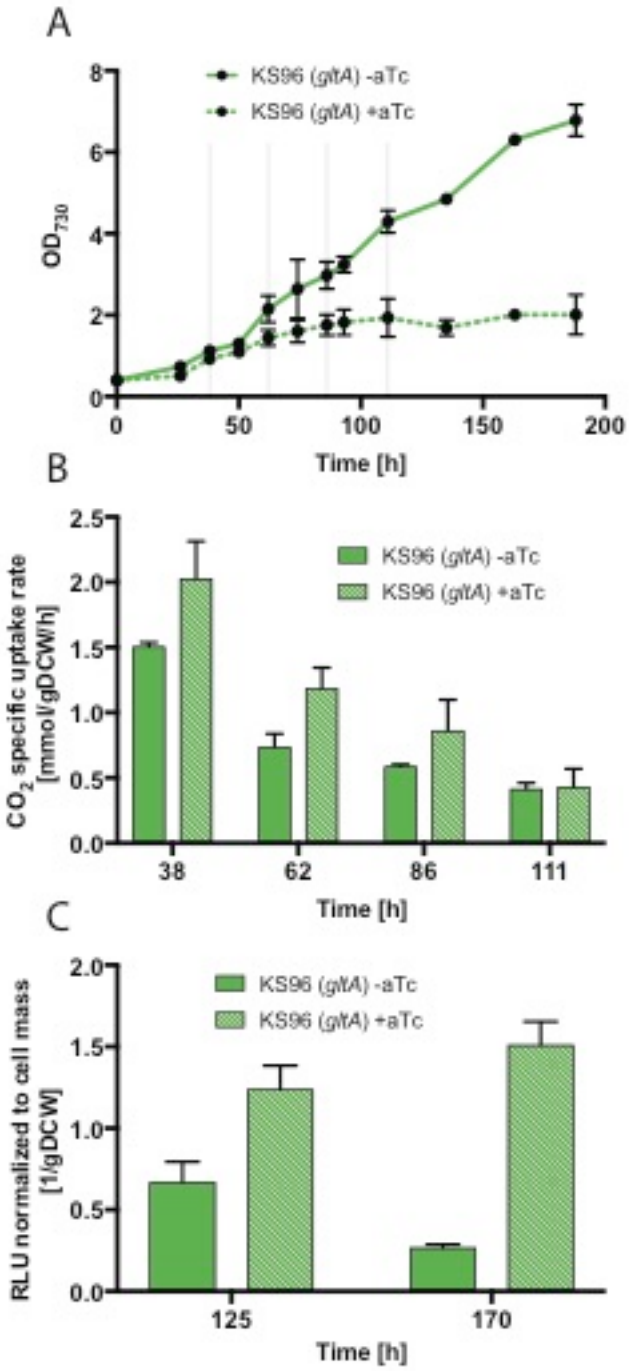

Figure 3. Growth, CO_2 uptake, and NADPH accumulation in KS96 (butanol-producing) during CRISPRi-mediated growth arrrest. Cells were grown in a batch photobioreactor. (A) Growth curve, where gray lines indicate when CO_2 uptake was measured. (B) Specific CO_2 uptake rate (biomass normalized). (C) Relative NADPH concentration as measured by luminescence assay (RLU relative light units). Cultures were inoculated at OD_{730} 0.1 in all cases. Repression of *gltA* was induced at culture start by addition of aTc. Butanol production was induced with IPTG at OD_{730} 0.4. Light intensity was 300 µE. Cultivations for CO_2 uptake rate were performed in duplicate. NADPH measurements were performed in triplicate.

Since strong *gltA* repression (>90% repressed) in KS96 led to total growth arrest and reduced CO_2 uptake, we tested partial repression of *gltA* as a way to potentially hinder growth while allowing significant CO_2 uptake. We designed new sgRNAs that would bind the *gltA* gene far from its transcription start site (TSS), resulting in different levels of *gltA* expression. The potency of gene repression by dCas9-sgRNA is weakened when the sgRNA binds far from the TSS.[25] We constructed sgRNA arrays containing sgRNA_*gltA*_463 (targeting 463 nt from TSS) and sgRNA_*gltA*_762 (targeting 762 nt from TSS). In this trial, the arrays also contained sgRNAs targeting subunits of the NAD(P)H dehydrogenase complex NDH-1 (*ndhD1D2*), acetate kinase (*ackA*), and PHB synthase (*phaEC*) (Table 1). These additional targets were predicted to enhance butanol synthesis.[26,27] The arrays were used to make KS142 and KS143, containing sgRNA_*gltA*_463 and sgRNA_*gltA*_762, respectively. KS142 and KS143 also contained the soluble transhydrogenase Sth from *P. aeruginosa* (Fig. S6).[28] KS87 served as a control strain as it contained an sgRNA array lacking *gltA* repression but was otherwise identical (Table 1).

We tested the growth and butanol production of the partial repression strains in a photobioreactor under a batch "photonfluxostat" regime, where the light intensity/OD is constant. This setup is intended to extend the exponential growth phase and allows more accurate calculation of specific productivity.[23] We found that growth of the three strains was not significantly different, indicating that *gltA* repression was not severe (Fig. 4A). In KS142 (*gltA*_463), specific butanol productivity (white bars in Fig. 4B) and butanol titers (Fig. 4C) were significantly higher than in KS87. In KS143 (*gltA*_762), butanol titers were significantly higher

than KS87, but specific productivity was not (two-way repeated measures ANOVA, $p<0.05$). Over the 4-day measurement period, carbon partitioning to butanol was on average 16% in KS142 (*gltA*_463), 11% for KS143 (*gltA*_762), and 9% for KS87 (*no sgRNA_gltA*) (Fig. 4B and Supplementary Note). Quantitative PCR of *gltA* mRNA levels showed that *gltA* was repressed 11% in KS142 and 15% in KS143, though the differences between the two strains were within the margin of error of the qPCR assay (Fig. S7). These results show that partial repression of *gltA* can increase butanol titers without affecting growth.

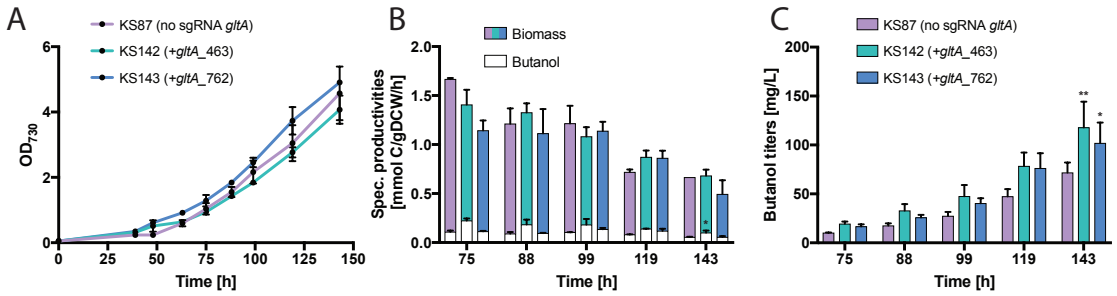

Figure 4. Carbon partitioning from biomass formation to butanol formation by partial repression of *gltA*. (A) Growth curve, (B) carbon partitioning, and (C) butanol titers. White bars in panel B indicate flux going to butanol whereas colored bars indicate flux going to biomass in C-mmol/gDCW/h. CRISPRi was induced with aTc in a pre-culture 4 days prior to experiment start. Strains were cultivated in the multicultivator in "photonfluxostat" mode with a light regime of 900 µmol photons m^{-2} s^{-2} OD_{720}^{-1}. Cultures were grown in duplicate. Two-way repeated measures ANOVA are denoted (* $p<0.05$; ** $p<0.005$).

We have shown that CRISPRi can be used as an effective tool to partition carbon flux between biomass and product in *Synechocystis.* Targeted repressions that affected metabolic branch points *and* arrested growth at an optimal cell density gave higher biofuel titers. Future efforts on two-phase production should focus on how to maintain a high CO_2 uptake and cell metabolism while growth is arrested. For instance, glucose uptake was improved in nitrogen-limited *E. coli* by modulating

the stringent response program, in effect removing the growth arrest signal.[29] A high substrate uptake must also be maintained over extended time periods to make two-stage fermentation processes successful.[30] The future success of growth-arrested strains will thus depend on understanding the mechanisms underlying decreased metabolic activity. For *Synechocystis*, one result of growth arrest is the accumulation of NADPH from the light reactions that is not used in biomass formation. Accumulation of NADPH could lead to a more reduced PQ pool,[31] which causes photo-inhibition and thus reduced CO_2 fixation. If the biofuel pathway does not carry enough flux, or does not utilize NADPH, reductant-dissipation valves may be necessary. An additional line of evidence supporting this is our observation that butanol-producing cultures, which generally carried less flux to product, became bleached earlier after the onset of growth repression than ethanol-producing cultures.

In this study, we have induced growth arrest via addition of an external inducer. In the future, both CRISPRi and pathways for biofuel production could be triggered by environmental signals, such as cellular density,[32] precursor accumulation,[33] light or nitrate concentration.[34] Fine-tuning a light-intensity circuit response[35] could ensure that growth suppression would occur when cell density is optimal. Cyanobacteria can also react to different light colors[36] and future indoor processes using LED lights[37] could involve switching light color to trigger production phase. Such a true "dynamic engineering" approach would also require a shorter delay time than reported here, likely through faster degradation of GltA once transcription is blocked.

249

Methods

Cyanobacteria cultivation

For the flask cultivations, mutant *Synechocystis* sp. PCC 6803 strains were cultivated at 30°C in a climatic chamber (Percival Climatics SE-1100), 100 μE/s/m^2 illumination, and 1 % v/v CO_2. Cultures were grown in BG-11 buffered to pH 7.8 and supplemented with the appropriate antibiotics. IPTG (1mM), to induce expression of nphT7, was added at OD_{730} 0.4. Induction of dCas9 and sgRNAs was with aTc added to 1μg/mL at OD_{730} 0.1 unless specified. Additional aliquots of aTc were added every two days. The multicultivator (Photon Systems Instruments) was run either in batch mode or 'photonfluxostat' (light regime factor 900 μmol photons m^{-2} s^{-2} OD_{720}^{-1}).[23] CO_2 from the outlet was measured online using a Cozir CM-0124 CO_2 sensor (CO2Meter.com). The CO_2 concentration difference between outlet and inlet and gas flow rate was used to calculate CO_2 uptake rate.

Constructs and strains

Synechocystis sp. PCC 6803 was a gift from Dr. Martin Fulda (Göttingen, Germany). All genes, promoters, terminators, and antibiotic resistance cassettes were assembled using Biobrick assembly. Biofuel production pathways were inserted at the *slr0168* locus (NSI), dCas9 at the *psbA2* (NSII) locus and the sgRNAs at the *slr2030* (NSIII) locus using pMD19-T targeting vector backbone (Takara). Strain genotypes were verified by colony PCR. A list of strains used for this study is available (Table 1 and Table S1).

Butanol and ethanol measurement

Cultures were pelleted at 13000 rpm for 10 min at 4°C. For butanol, 300 µL supernatant was mixed vigorously with 100 µL dichloromethane for 30 s. Isobutanol (5 µL, 0.1%) was used as internal standard. For ethanol, 80 µL supernatant was mixed with 80 µL acetonitrile. Butanol (10 µL, 0.1%) was used as internal standard. Both ethanol and butanol were quantified through GC-FID (Shimadzu GC2010 Plus) using a Stabilwax column (30 m x 0.25 mm ID, 0.25 µm film thickness, RESTEK).

Minimization of Metabolic Adjustment (MOMA)

We used an updated version[26] of the iJN678 genome-scale model.[19] Minimization of metabolic adjustment (MOMA) was performed using the OptFlux software[38] to predict flux distributions of mutant strains.[39] FBA was performed using the COBRA toolbox 2.0[40] on MATLAB (Mathworks Inc.).

Design of sgRNAs

We used an in-house Python script to find potential sgRNAs inside a given ORF. The algorithm made sure to select sgRNAs without unwanted off-target bindings, absence of Biobrick restriction sites in the sequence, absence of terminators, as well as additional stability criteria. A list of sgRNAs used in this study is available in the supplemental (Table S2).

RT-qPCR

Total RNA was isolated from 4 mL of *Synechocystis* culture (OD_{730} = 1.0-3.0) using the GeneJet RNA purification kit (Thermo Fisher). Manufacture's instructions were followed except that lysozyme was added to the TE buffer to 40 mg/L instead of 0.4 mg/L. Beads were also used to lyse the cells. DNA was removed using the RapidOut DNA Removal Kit (Thermo Fisher). RT-qPCR was performed on 50–100 ng of total RNA with the Power SYBR Green RNA-to-Ct kit (Thermo Fisher) and a BioRad CFX light cycler. Reference gene *rpoB* (*sll1787*) was used as internal standard. Appropriate no-RT controls were also included.

NADPH quantification

Cultures (10ml) were pelleted at 4000 g for 10 min at 4°C. The pellets were resuspended in 200 µL cold 0.2 M NaOH + 1 % (w/V) DTAB. Glass beads were added (100 µL), samples were vortexed for 30 min at 4°C and centrifuged at 13000 rpm for 10 min at 4°C. The supernatants were analysed with the NADP/NADPH-Glo Assay Kit (Promega) according to the manufacturer's protocol.

Supporting Information: A file containing supplementary table and figures (PDF).

Author contributions

KS and EPH proposed the idea, designed the experiments and wrote the paper. KS and EL performed the experiments. JA designed the butanol pathway and established product quantification. MJ set up the multicultivator and CO_2 sensors. LY provided the dCas9 strains. EPH supervised. All authors read and approved the final manuscript.

The authors declare no financial competing interest.

Acknowledgements

This work was supported by the Swedish Research Council Formas (213-2011-1655), the Swedish Foundation for Strategic Research (RBP14-0013) and the EU Horizon 2020 Research and Innovation Program (ENGICOIN No. 760994).

References

(1) Brockman, I. M., and Prather, K. L. J. (2015) Dynamic metabolic engineering: New strategies for developing responsive cell factories. *Biotechnol. J 10*, 1360–1369.
(2) Venayak, N., Anesiadis, N., Cluett, W. R., and Mahadevan, R. (2015) Engineering metabolism through dynamic control. *Curr. Opin. Biotechnol. 34*, 142–152.
(3) Lynch, M. D. (2016) Into new territory: Improved microbial synthesis through engineering of the essential metabolic network. *Curr. Opin. Biotechnol. 38*, 106–111.
(4) Cho, H. S., Seo, S. W., Kim, Y. M., Jung, G. Y., and Park, J. M. (2012) Engineering glyceraldehyde-3-phosphate dehydrogenase for switching control of glycolysis in escherichia coli. *Biotechnol. Bioeng. 109*, 2612–2619.
(5) Soma, Y., Tsuruno, K., Wada, M., Yokota, A., and Hanai, T. (2014) Metabolic flux redirection from a central metabolic pathway toward a synthetic pathway using a metabolic toggle switch. *Metab. Eng. 23*, 175–184.
(6) Brockman, I. M., and Prather, K. L. J. (2015) Dynamic knockdown of E. coli central metabolism for redirecting fluxes of primary metabolites. *Metab. Eng. 28*, 104–113.
(7) Yuan, J., and Ching, C. B. (2015) Dynamic control of ERG9 expression for improved amorpha-4,11-diene production in Saccharomyces cerevisiae. *Microb. Cell Fact. 14*, 1–10.
(8) Li, S., Jendresen, C. B., Grünberger, A., Ronda, C., Jensen, S. I., Noack, S., and Nielsen, A. T. (2016) Enhanced protein and biochemical production using CRISPRi-based growth switches. *Metab. Eng. 38*, 274–284.
(9) Straka, L., and Rittmann, B. E. (2017) Effect of culture density on biomass production and light utilization efficiency of Synechocystis sp. PCC 6803. *Biotechnol. Bioeng. 115*, 507–511.
(10) Kopka, J., Schmidt, S., Dethloff, F., Pade, N., Berendt, S., Schottkowski, M., Martin, N., Dühring, U., Kuchmina, E., Enke, H., Kramer, D., Wilde, A., Hagemann, M., and Friedrich, A. (2017) Systems analysis of ethanol production in the genetically engineered cyanobacterium Synechococcus sp. PCC 7002. *Biotechnol. Biofuels 10*, 56.
(11) Yao, L., Cengic, I., Anfelt, J., and Hudson, E. P. (2016) Multiple Gene Repression in Cyanobacteria Using CRISPRi. *ACS Synth. Biol. 5*, 207–212.

(12) Gordon, G. C., Korosh, T. C., Cameron, J. C., Markley, A. L., Begemann, M. B., and Pfleger, B. F. (2016) CRISPR interference as a titratable, trans-acting regulatory tool for metabolic engineering in the cyanobacterium Synechococcus sp. strain PCC 7002. *Metab. Eng. 38*, 170–179.
(13) Kaczmarzyk, D., Cengic, I., Yao, L., and Hudson, E. P. (2018) Diversion of the long-chain acyl-ACP pool in Synechocystis to fatty alcohols through CRISPRi repression of the essential phosphate acyltransferase PlsX. *Metab. Eng. 45*, 59–66.
(14) Huang, C. H., Shen, C. R., Li, H., Sung, L. Y., Wu, M. Y., and Hu, Y. C. (2016) CRISPR interference (CRISPRi) for gene regulation and succinate production in cyanobacterium S. elongatus PCC 7942. *Microb. Cell Fact. 15*, 196.
(15) Anfelt, J., Kaczmarzyk, D., Shabestary, K., Renberg, B., Uhlen, M., Nielsen, J., and Hudson, E. P. (2015) Genetic and nutrient modulation of acetyl-CoA levels in Synechocystis for n-butanol production. *Microb. Cell Fact. 14*, 167.
(16) Lan, E. I., and Liao, J. C. (2012) ATP drives direct photosynthetic production of 1-butanol in cyanobacteria. *Proc. Natl. Acad. Sci. 109*, 6018–6023.
(17) Heo, M. J., Jung, H. M., Um, J., Lee, S. W., and Oh, M. K. (2017) Controlling Citrate Synthase Expression by CRISPR/Cas9 Genome Editing for n-Butanol Production in Escherichia coli. *ACS Synth. Biol. 6*, 182–189.
(18) Koropatkin, N. M., Pakrasi, H. B., and Smith, T. J. (2006) Atomic structure of a nitrate-binding protein crucial for photosynthetic productivity. *Proc. Natl. Acad. Sci. 103*, 9820–9825.
(19) Nogales, J., Gudmundsson, S., Knight, E. M., Palsson, B. O., and Thiele, I. (2012) Detailing the optimality of photosynthesis in cyanobacteria through systems biology analysis. *Proc. Natl. Acad. Sci. 109*, 2678–2683.
(20) Huang, H.-H., and Lindblad, P. (2013) Wide-dynamic-range promoters engineered for cyanobacteria. *J. Biol. Eng. 7*, 10.
(21) Landry, B. P., Stöckel, J., and Pakrasi, H. B. (2013) Use of degradation tags to control protein levels in the cyanobacterium Synechocystis sp. strain PCC 6803. *Appl. Environ. Microbiol. 79*, 2833–2835.
(22) Albers, E., Larsson, C., Andlid, T., Walsh, M. C., and Gustafsson, L. (2007) Effect of nutrient starvation on the cellular composition and metabolic capacity of Saccharomyces cerevisiae. *Appl. Environ. Microbiol. 73*, 4839–4848.
(23) Du, W., Jongbloets, J. a., Pineda Hernãndez, H., Bruggeman, F. J., Hellingwerf, K. J., and Branco dos Santos, F. (2016) Photonfluxostat: A method for light-limited batch cultivation of cyanobacteria at different, yet constant, growth rates. *Algal Res. 20*, 118–125.
(24) Ducat, D. C., Avelar-Rivas, J. A., Way, J. C., and Silver, P. A. (2012) Rerouting carbon flux to enhance photosynthetic productivity. *Appl. Environ. Microbiol. 78*, 2660–2668.
(25) Qi, L. S., Larson, M. H., Gilbert, L. A., Doudna, J. A., Weissman, J. S., Arkin, A. P., and Lim, W. A. (2013) Repurposing CRISPR as an RNA-guided platform for sequence-specific control of gene expression. *Cell 152*, 1173–1183.
(26) Shabestary, K., and Hudson, E. P. (2016) Computational metabolic engineering strategies for growth-coupled biofuel production by Synechocystis. *Metab. Eng. Commun. 3*, 216–226.
(27) Erdrich, P., Knoop, H., Steuer, R., and Klamt, S. (2014) Cyanobacterial biofuels:

406 new insights and strain design strategies revealed by computational modeling.
407 *Microb. Cell Fact. 13*, 128.
408 (28) Angermayr, S. A., Paszota, M., and Hellingwerf, K. J. (2012) Engineering a
409 cyanobacterial cell factory for production of lactic acid. *Appl. Environ. Microbiol. 78*,
410 7098–7106.
411 (29) Michalowski, A., Siemann-herzberg, M., and Takors, R. (2017) Escherichia coli
412 HGT : Engineered for high glucose throughput even under slowly growing or resting
413 conditions. *Metab. Eng. 40*, 93–103.
414 (30) Klamt, S., Mahadevan, R., and Hädicke, O. (2017) When Do Two-Stage Processes
415 Outperform One-Stage Processes ? *Biotechnol. J. 13*.
416 (31) Keren, N., and Krieger-Liszkay, A. (2011) Photoinhibition: Molecular
417 mechanisms and physiological significance. *Physiol. Plant. 142*, 1–5.
418 (32) Basu, S., Mehreja, R., Thiberge, S., Chen, M.-T., and Weiss, R. (2004)
419 Spatiotemporal control of gene expression with pulse-generating networks. *Proc.*
420 *Natl. Acad. Sci. 101*, 6355–60.
421 (33) Rogers, J. K., Taylor, N. D., and Church, G. M. (2016) Biosensor-based
422 engineering of biosynthetic pathways. *Curr. Opin. Biotechnol. 42*, 84–91.
423 (34) Immethun, C. M., DeLorenzo, D. M., Focht, C. M., Gupta, D., Johnson, C. B., and
424 Moon, T. S. (2017) Physical, Chemical, and Metabolic State Sensors Expand the
425 Synthetic Biology Toolbox for Synechocystis sp. PCC 6803. *Biotechnol. Bioeng. 114*,
426 1561–1569.
427 (35) Ang, J., Harris, E., Hussey, B., Krill, R., and McMillen, D. R. (2013) Tuning
428 Biological Response Curves for Synthetic Biology. *ACS Synth. Biol. 2*, 547–567.
429 (36) Chau, R. M. W., Bhaya, D., and Huang, K. C. (2017) Emergent phototactic
430 responses of cyanobacteria under complex light regimes. *MBio 8*, 1–15.
431 (37) Lips, D., Schuurmans, J. M. M., Branco dos Santos, F., and Hellingwerf, K. J.
432 (2017) Many ways towards "solar fuel": Quantitative analysis of the most promising
433 strategies and the main challenges during scale-up. *Energy Environ. Sci. 11*, 10–22.
434 (38) Rocha, I., Maia, P., Evangelista, P., Vilaça, P., Soares, S., Pinto, J. P., Nielsen, J.,
435 Patil, K. R., Ferreira, E. C., and Rocha, M. (2010) OptFlux: an open-source software
436 platform for in silico metabolic engineering. *BMC Syst. Biol. 4*, 45.
437 (39) Segrè, D., Vitkup, D., and Church, G. M. (2002) Analysis of optimality in natural
438 and perturbed metabolic networks. *Proc. Natl. Acad. Sci. 99*, 15112–15117.
439 (40) Schellenberger, J., Que, R., Fleming, R. M., Thiele, I., Orth, J. D., Feist, A. M.,
440 Zielinski, D. C., Bordbar, A., Lewis, N. E., Rahmanian, S., Kang, J., Hyduke, D. R., and
441 Palsson, B. O. (2011) Quantitative prediction of cellular metabolism with constraint-
442 based models: the COBRA Toolbox. *Nat. Protoc. 6*, 1290–1307.
443
444